Colloids and Surfaces B: Biointerfaces 76 (2010) 241–247

Contents lists available at ScienceDirect

Colloids and Surfaces B: Biointerfaces

journal homepage: www.elsevier.com/locate/colsurfb

The role of protein binding in the poisoning of gold nanoparticle catalysts

Yan Chen[1], Kaleyhia Flowers, Milagros Calizo, Sandra Whaley Bishnoi*

Illinois Institute of Technology, Department of Biological, Chemical, and Physical Sciences, 3101 South Dearborn Street, Chicago, IL 60616, United States

ARTICLE INFO

Article history:
Received 11 September 2009
Accepted 29 October 2009
Available online 6 November 2009

Keywords:
Nanoparticle
Enzyme catalysis
Colloidal gold
Nucleation
Protein adsorption
Bovine serum albumin
Glucose oxidase

ABSTRACT

Seed mediated catalytic growth of gold nanoparticles is used in the design of biosensors for the products of peroxidase proteins, though the role of *in situ* proteins and the enzymes themselves on the sensitivity of these biosensors is yet to be addressed. This work specifically focuses on whether the presence of proteins with a strong attraction to the gold nanoparticle seeds, such as albumin proteins, inhibits the nanoparticle's catalytic properties. We have determined that the sensitivity of the biosensor design, defined as its response to the reducing agent hydrogen peroxide, is highly dependent on the presence of bovine serum albumin (BSA) and less dependent on the presence of the enzyme glucose oxidase. We suggest that the strong interaction between BSA and the gold surface leads to poisoning of the catalytic sites on the particle surface, which reduces the uniform growth of the nanoparticles and increases asymmetric growth of small gold nanoparticles onto the seed surface. The overall effect of the protein interaction is to lower the sensitivity of the model biosensor.

1. Introduction

The application of metal nanoparticles in the design of biosensors is increasingly frequent [1–3]. One common embodiment uses the shift in plasmon resonance from the aggregation of particles upon the addition of analyte to determine the concentration of analyte present [4–6]. In addition, several groups have taken advantage of nanoparticle seed mediated growth to develop biosensors for use in detecting the products of enzymes, such as the growth of gold nanoparticles to detect the hydrogen peroxide produced by oxidases [7–11], or indicators of reactions, such as the growth of silver nanoparticles through α-NADPH-dependent nitrate reductase with phytochelatin [12]. Additionally, the growth of nanoparticles using silver staining methods has also been used to improve the detection limits of biosensors which use nanoparticles for DNA detection [13].

Much has been explored about how to control the size and morphology of nanoparticles during solution synthesis [14–17], including the importance of controlling growth kinetics [18,19], pH of growth solutions [20], and the presence of capping agents [21–24]. The use of biologically relevant species, such as peptides [25–30], enzyme cofactors [31], and proteins [32], during the synthesis of nanoparticles has become more common to produce nanoparticles with water stability and biological functionality. Often the resulting nanoparticles produced with these biological species are smaller than those produced without any capping agents, but similar to those produced using alkanethiol capping agents [31]. However, little has been explored regarding how the presence of these biological species will affect the seed mediated growth of nanoparticles used in biosensors. Since serum albumin proteins are among the most abundant proteins present in plasma (normal levels are 34–50 g/L) [33], we have specifically focused on the how this protein might affect seed mediated growth in a model biosensor. In this work, we compare the effect of serum albumin, a protein known to have a high affinity for gold [32,34–37], to the presence of glucose oxidase on a model biosensor's sensitivity to the presence of a reducing agent. In addition, we investigate how the shape of particles formed by seed mediated growth is affected by the presence of high affinity proteins.

2. Experimental

2.1. Chemicals and materials

Bovine serum albumin (BSA), trisodium citrate, glucose oxidase from *Aspergillus niger* (201 U/mg), chloroauric acid ($HAuCl_4$), tetrakis(hydroxymethyl) phosphonium chloride (THPC), and hydrogen peroxide (H_2O_2) are obtained from Sigma Chemical Co. and used without further purification. The stock solution of H_2O_2 is freshly diluted from 30 wt% in water (9.8 M) to 8 mM with ultrapure water (Milli-Q) purified by a Millipore system.

* Corresponding author. Tel.: +1 312 567 8922; fax: +1 312 567 3494.
E-mail address: bishnoi@iit.edu (S.W. Bishnoi).
[1] Present address: Department of Environmental and Chemical Engineering, Yanshan University, Qinhuangdao, 438 East Hebei Street, Qinhuangdao 066004, PR China. Tel.: +86 335 8061569.

0927-7765/$ – see front matter © 2009 Elsevier B.V. All rights reserved.
doi:10.1016/j.colsurfb.2009.10.043

2.2. High resolution transmission electron microscopy

Transmission electron microscopy (TEM) images are acquired with a JEOL 3010 electron microscope (University of Illinois at Chicago, Research Resource Center). Due to the low concentration of particles in solution, centrifugation is required to concentrate the solutions prior to deposition onto the TEM grid. The particle solutions are centrifuged for 5 min at 10,000 rpm and the supernatant is then decanted until the concentration is ~10-fold greater than the as-prepared solution. After sonication for 10 min, 30 μL of the concentrated particle solution is placed on a carbon-coated copper grid and evaporated at room temperature prior to analysis on the microscope.

2.3. Dynamic light scattering

All dynamic light scattering (DLS) measurements were collected using a Malvern Nano-S instrument (Malvern Instrument, UK). The measurement (cell) position and attenuation settings were optimized for the as-synthesized gold colloid particles (measurement position = 4.65, Attenuator index = 8). These settings were maintained throughout the subsequent particle growth measurements to allow count rates to be compared. The measurement position was 4.65 mm from the cell wall of a 12 mm cuvette. The size was reported as a *Z*-average size, also known as the Cumulants mean. The *Z*-average is calculated from the signal intensity, which is based on the cumulants analysis. The cumulants analysis is the fit of a polynomial to the log of the G1 correlation function using Eq. (1) [38]. The value of *b*, the second order cumulant, is converted to a size using the dispersant viscosity and instrumental constants. The volume corrected mean (which takes into account the refractive index and absorption of the particles in solution) has also been provided to take into account that the intensity mean is dominated by the presence of a small number of large particles (the scattering intensity of a particle is proportional to diameter to the sixth power according to Rayleigh's approximation) [39]. The analysis model used was the "General Purpose" model provided by the Malvern Dispersion Technology Software Version 5.10.

$$\ln[G1] = a + bt + ct^2 + dt^3 + et^4 + \cdots \quad (1)$$

2.4. Preparation of Au-NP seeds

Gold nanoparticles (stabilized by citrate) are prepared following Frens' method [20] using sodium citrate to reduce chloroauric acid. Typically, a 100 mL aqueous solution of 0.01% $HAuCl_4$ is heated to boiling, and then 2 mL of 1% sodium citrate added. The mixture is stirred until a wine red color is obtained, cooled to room temperature, and then stored in the refrigerator until needed. Particle size (~20 nm) is measured by DLS. The gold colloid concentration is calculated to be about 9.93×10^{-10} M using an extinction coefficient of $1.03 \times 10^9\ M^{-1}\ cm^{-1}$ and the absorbance of the solution at 506 nm (JASCO V-530 UV–vis spectrometer), according to the method provided by Liu et al. [40]. Another gold nanoparticle solution used in the experiment is THPC–gold (~6 nm diameter). Briefly, 4 mL of a stock solution of tetrakis(hydroxymethyl)phosphonium chloride (THPC) (400 μL into 33 mL of Milli-Q water) is added into 180 mL of 6.6×10^{-3} M NaOH solution [41]. The solution is stirred for 5 min and then 6.75 mL of 1% chloroauric acid is rapidly added into the vortexing solution. The color changes instantly to a light brown and is aged in the refrigerator for at least 24 h prior to use as a seed particle. The concentration of THPC–gold was calculated to be approximately 6.08×10^{-8} M using an extinction coefficient of $1.89 \times 10^7\ M^{-1}\ cm^{-1}$ and the absorbance of the solution at 506 nm [40]. The final particle size according to DLS was found to be ~6 nm.

2.5. Catalytic growth of Au-NPs

To determine the role that bovine serum albumin (BSA) plays in the growth reaction, BSA is dissolved in phosphate-buffer solution (PB, 0.01 M, pH 7) at different concentrations from zero to 904 μg/mL. The growth solution consists of 1.62 mL of gold nanoparticle solution, either 5.65×10^{-11} M gold colloid or 6.82×10^{-9} M THPC–gold to maintain similar surface areas, and 0.75 mL of BSA in PB. This solution is mixed with different concentrations of H_2O_2 (total volume 1 mL), allowed to incubate for 3 min prior to the addition of 28.62 μL of $HAuCl_4$ (final concentration = 2.4×10^{-4} M $HAuCl_4$). The absorbance spectra are recorded by UV–vis spectroscopy after a fixed time interval of 10 min to maintain reproducibility of the measurements. DLS measurements are also taken exactly 10 min after the initiation of the reaction. All experimental procedures and measurements are performed at room temperature (25 °C). The final concentration of BSA ranges from 0 to 200 μg/mL. Additional UV–vis measurements are taken at longer intervals to determine how adsorption of BSA affects the rate of catalytic growth (Supplementary material).

For comparison, the BSA used in the above reaction is replaced with glucose oxidase (GOx, MW = 160,000 Da) from *Aspergillus niger* dissolved in PB. GOx is a commonly used enzyme for detecting the presence of glucose in nanoparticle based sensors [8,9,42]. The final concentration of GOx ranges from 0 to 600 μg/mL.

3. Results and discussion

Since BSA is known to bind strongly to gold surfaces, especially those with a citrate coating [34,36,43], we investigated how these interactions between BSA and NP seeds affect particle growth and therefore the sensitivity of a model biosensor. Fig. 1 shows the absorbance spectra of the growth solutions in the presence of different concentrations of H_2O_2 and BSA. No reaction is observed between hydrogen peroxide and Au ions in the absence of the gold seed particles within the 10 min incubation period, demonstrating the role of the gold nanoparticle (NP) seeds as catalysts in the reaction. The overall particle extinction is expected to increase with the addition of H_2O_2, which reduces the chloroauric acid onto the surface of gold NP seeds until the point when all of the excess Au(III) ions provided have been consumed [8]. This is the same effect observed by others using NPs as seeds in enzymatic reactions [8,9,44]. As has been observed previously, the initial red shift observed at low H_2O_2 concentrations supports the concept of particle enlargement; however, a blue-shift is seen at higher H_2O_2 concentrations due to the formation a mixture of very small crystalline Au-NPs together with enlarged Au-NPs [7,8]. However, when even a small amount of BSA is added to the reaction solution (50 μg/mL), the narrow, blue-shifted peaks seen at high $[H_2O_2]$ are no longer present. At higher concentrations of BSA (200 μg/mL), the overall extinction of the particles increases only slightly and the shape of the peak is similar to that seen before the addition of H_2O_2. This result reveals that the presence of BSA affects the seed mediated growth reaction.

In an attempt to quantify the observations in Fig. 1a, we examined the "sensitivity" of catalytic reactions as a function of the concentration of BSA. We define "sensitivity" as the slope of the change in the particle solutions' absorbance at 523 nm (wavelength of maximum absorption for original particle solution) with increasing hydrogen peroxide concentration, or $\Delta A_{523\,nm}/[H_2O_2]$, according to the linear least squares regressions shown in Fig. 1d–f. According to Beer's law, the absorbance of a gold NP solution in UV–vis spectroscopy is related to the concentration of gold NPs and the extinction coefficient of the NPs, which is dependent on a particle's size [40]. Though it is clear that the relationship is not truly

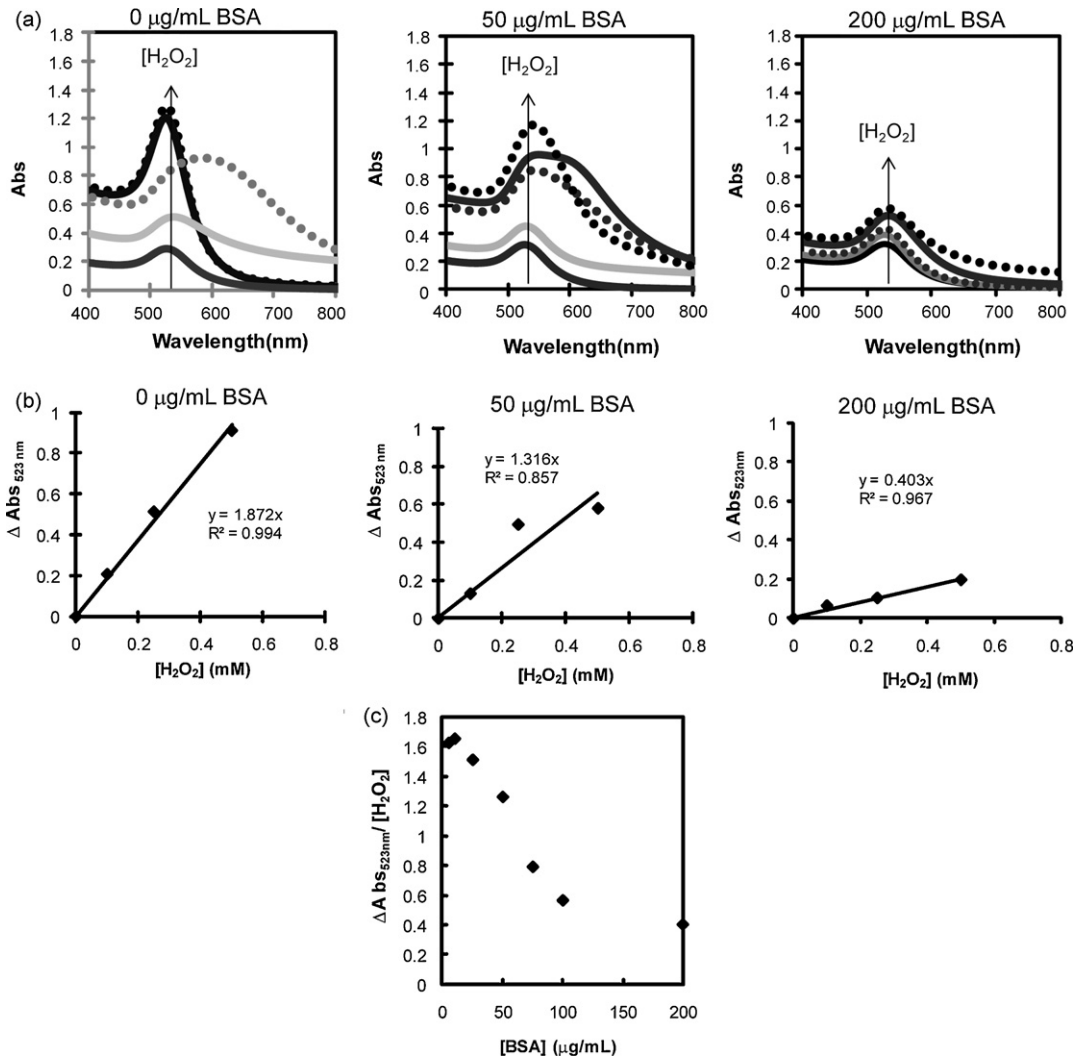

Fig. 1. (a) Absorbance spectra of Au-colloid (20 nm) seed in the presence of $HAuCl_4$ in 0.01 M phosphate-buffer solution of pH 7 as the function of concentration of H_2O_2 (from bottom to top, 0, 0.1, 0.25, 0.5, and 1.0 mM H_2O_2) at three different BSA concentrations, 0, 50, and 200 μg/mL. (b) The resulting response curves are plotted below for each concentration. (c) The overall change in "sensitivity" ($\Delta A_{523\,nm}/[H_2O_2]$) as a function of [BSA] added.

"linear" for some solutions (namely 50 μg/mL BSA), this provides a more quantitative method for tracking the effects of BSA on particle growth. From the response curves (Fig. 1b), it is apparent that the sensitivity of this type of enzymatic reaction is dependent on the presence of proteins that have a strong affinity to the gold surface, since increasing the concentration of BSA used in the reaction to 200 μg/mL caused an approximately 5× decrease in the sensitivity of the response curve (Fig. 1c). This concentration corresponds to roughly 2×10^{12} molecules/cm^2, which is less than monolayer coverage (3×10^{12} molecules/cm^2) according to previous studies with citrate-stabilized gold surfaces [34].

A linear least squares regression of the change in absorbance for a fixed wavelength (523 nm) only provides a semi-quantitative measure of the differences between NP solutions with and without BSA added, because of bathochromic shifts in the spectra upon addition of H_2O_2 and saturation at high $[H_2O_2]$ (due to the complete consumption of gold ions), which limit the linearity of the response. If the area under the curve is plotted versus $[H_2O_2]$ (Supplementary material), the linearity of response is now even more limited and confined to low hydrogen peroxide concentrations (<0.25 mM), except for solutions containing [BSA] over 50 μg/mL. Using the magnitude of the slope of ΔArea versus $[H_2O_2]$, the onset of particle growth inhibition is ~25 μg/mL of BSA (~2.7×10^{11} BSA molecules/cm^2), corresponding to approximately one-tenth of a monolayer and ~1.3 BSA molecules per particle (Supplementary material) [34].

Though the addition of BSA appears to hinder the initial sensitivity of the model biosensor, the overall area under the curve actually increases with the addition of <100 μg/mL BSA at higher H_2O_2 concentrations (>0.25 mM) compared to solutions without BSA. The source of this increase in area is most likely due to a reduction in the detachment of nanoclusters from the surface of the seed particles. This idea is supported by both light scattering (Fig. 2) and transmission electron microscopy (Fig. 3) measurements. For Au NP solutions with BSA ≤ 10 μg/mL, the hydrodynamic diameter (D_H) decreases with increasing concentrations of H_2O_2, which correlates well with the blue-shift seen in the UV–vis spectra at higher hydrogen peroxide concentrations (Fig. 1). In addition, the count rate (Fig. 2b) continues to increase dramatically upon addition of large amounts of hydrogen peroxide in solutions where BSA is <25 μg/mL (Fig. 2b), while the count rate only increases marginally for those solutions containing more BSA. This observation agrees with previous studies that suggest that light scattering provides a sensitive detection method for the quantification of glucose by seed mediated growth of nanoparticles [7].

Fig. 3 shows the TEM results of gold colloid after 10 min of reacting with H_2O_2 (0.25 and 1 mM) and BSA (0–200 μg/ml). When hydrogen peroxide is added, Au crystallites are catalytically grown

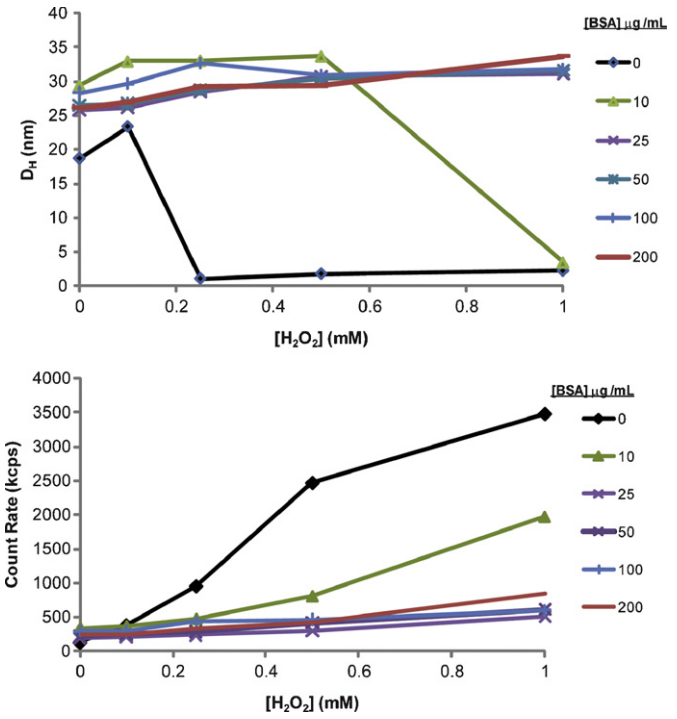

Fig. 2. (a) Resulting hydrodynamic diameter (D_H) for the seed solutions after reduction of additional Au(III) with H_2O_2 as measured by dynamic light scattering. (b) Measured count rate from light scattering as a function of [H_2O_2] and [BSA] added to the seed solutions.

on the faces of the parent Au seeds and should ideally form a uniform layer of gold on the NP surface. However, previous studies by Zayats et al. [8] using 13 nm particles showed that in addition to overall nanoparticle growth, Au nanoclusters are formed on the particle surface which can detach from the larger seed particles, contributing to the blue-shift of the absorbance spectra at high H_2O_2 concentration. NPs without the presence of BSA are shown to be initially aggregated (Fig. 3a) but separate into individual large particles (~80 nm) with increasing amounts of hydrogen peroxide (Fig. 3d). The initial aggregation may occur from placing the particles into a phosphate-buffer solution with chloroauric acid prior to the addition of hydrogen peroxide. However, since only limited aggregation was seen in DLS measurements prior to the addition of reducing agent (Fig. 2a), it likely that the aggregation seen in the initial TEM images is due to the centrifugation step used to concentrate the particles prior to TEM analysis.

Interestingly, Fig. 3 shows quite a difference in the gold NP's morphology at high concentrations of hydrogen peroxide in the presence of BSA (Fig. 3e and f) versus particles without BSA (Fig. 3d). First, the degree of aggregation seen in Fig. 3e and f is significantly greater than that shown without the presence of BSA (Fig. 3d). Second, though there were large aggregates, the size of the individual particles making up those aggregates do not change significantly (Supplementary material Table 2). Third, the formation of numerous separate nodes of various sizes was observed on the surface of gold seeds (Fig. 3b, c, e and f). These nodes are similar to the nanodendrite structures found when bimetallic Pd–Pt nanostructures are created from truncated octahedral Pd seeds [45]. These small nodes may contribute to the weak but gradual increase of the absorbance spectra with increasing the concentration H_2O_2 and the lack of shift in the wavelength of absorbance maxima in the absorbance spectra (Fig. 1a). The TEM results imply that when BSA binds to the surface [34], it blocks biocatalytic growth sites on the surface of gold, forcing additional gold deposition onto any uncovered sites and thereby non-uniform growth of the NP seeds (Scheme 1). These results also suggest that the presence of BSA allows the nanoclusters formed on the particles to maintain their association with the parent seed particles.

In order to determine whether this effect is dependent on the particle's surface chemistry and size, an additional nanoparticle catalyst is tested in the model biosensor. Instead of using citrate reduced gold colloid, the significantly smaller gold NP (THPC–gold, diameter ~6 nm) produced using alkaline solutions of tetrakis(hydroxymethyl) phosphonium chloride (THPC) as the reducing agent [41] is tested. These particles have been shown to have some phosphorous component on their surfaces and were therefore expected to show differences in their ability to catalyze

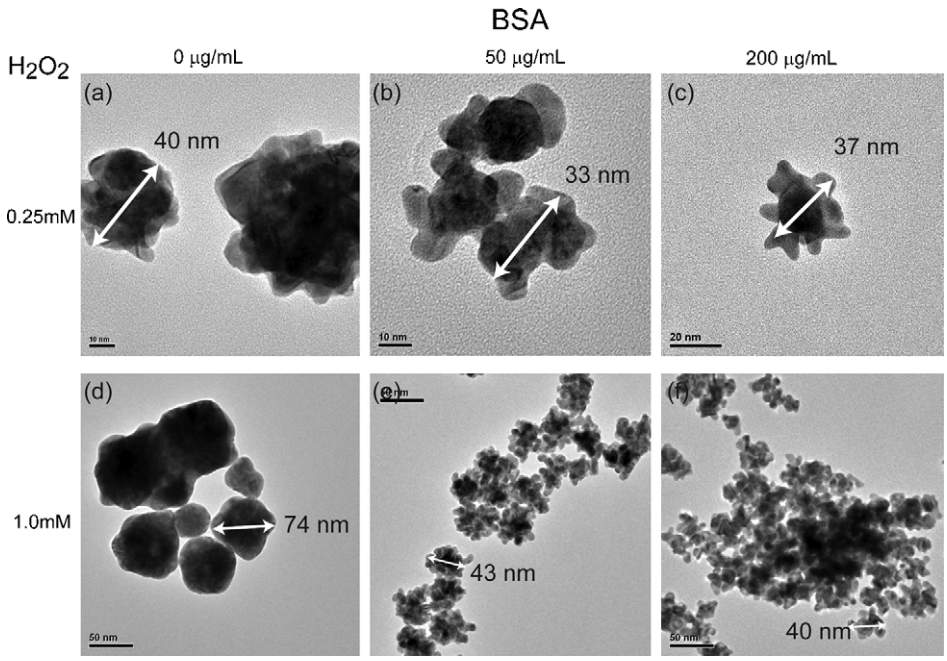

Fig. 3. TEM images of gold NP growth in the presence of 2×10^{-4} M $HAuCl_4$ and varying concentrations of H_2O_2 (0.25 and 1.0 mM) at the different BSA concentrations (0–200 μg/mL).

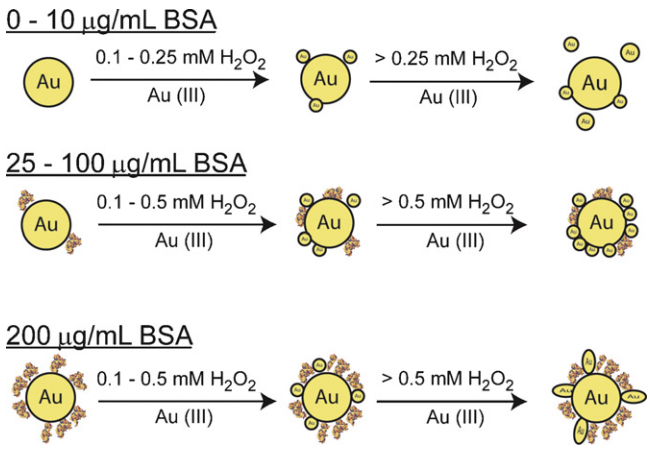

Scheme 1. Proposed model of biocatalytic growth of Au-NPs in the presence and absence of BSA.

the reaction between gold ions and hydrogen peroxide and their affinity to BSA. Fig. 4 shows the absorbance of the THPC–gold NPs after the addition of H_2O_2 in the presence of varying concentrations of BSA. Our first observation is that THPC–gold nanoparticles behave remarkably similar as NP catalysts as those produced using the citrate reduction method. Second, the sensitivity of THPC–gold dramatically decreases with increasing concentration of BSA (Fig. 4b–c). When the concentration of BSA is increased from 0 to 200 μg/ml, the sensitivity is reduced from 1.4 a.u./mM down to 0.04 a.u./mM H_2O_2 (THPC–gold, Fig. 4c). When area under the curve is used as a measurement of biosensor inhibition by BSA instead of the change in absorbance at a fixed wavelength, similar results were seen for THPC–gold particles as found with Au-colloid particles (Supplementary information). The main differences between the way these two particles behave in the presence of BSA is that there is not clear inhibition of the biosensor response for THPC–gold nanoparticles until the BSA concentration reaches a concentration of 75 μg/mL, whereas inhibition for begins at approximately 25 μg/mL for the Au-colloid nanoparticles. This difference most likely resides in the difference between the two particle sizes and their concentration in solution. When the change in the initial response of the model biosensors is compared (i.e. low [H_2O_2]), it is clear that response for the THPC–gold particles actually increases at low BSA concentrations while the Au-colloid particles decline upon the addition of any BSA (Supplementary material). The critical concentration that poisons both model biosensors is 200 μg/mL, which corresponds to a BSA:Au ratio of 1:1 for THPC–gold and 100:1 for Au-colloid particles. Overall, these results indicate that the presence of BSA hinders the catalytic reaction for both types of particles but that the response is a function of particle size and concentration.

Finally, we tested whether the seed mediated growth process is affected by incubation with the actual peroxidase enzyme that is

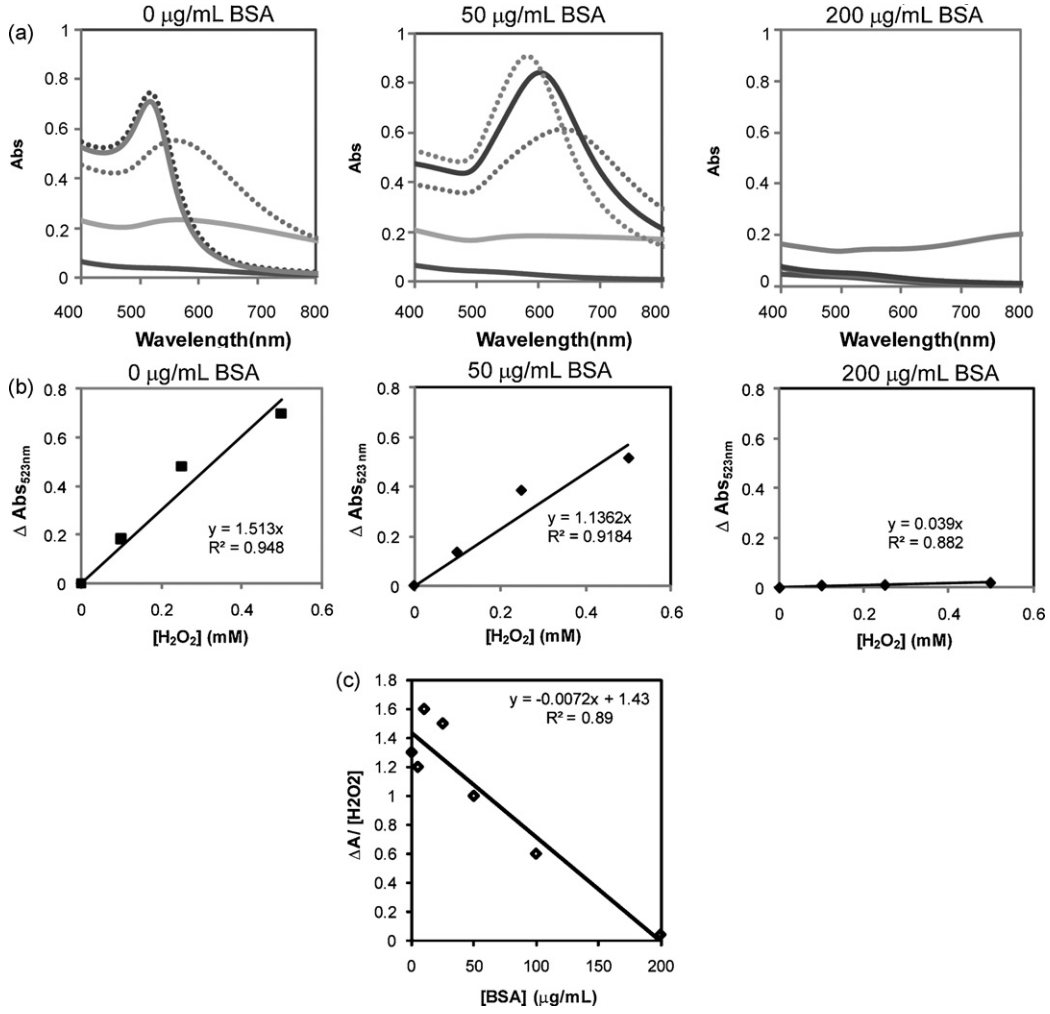

Fig. 4. (a) Absorbance spectra of THPC–gold (6 nm) seed in the presence of $HAuCl_4$ in 0.01 M phosphate-buffer solution of pH 7 as the function of concentration of H_2O_2 (from bottom to top, 0, 0.1, 0.25, 0.5, and 1.0 mM H_2O_2) at three different BSA concentrations, 0, 50, and 200 μg/mL. (b) The resulting response curves are plotted below for each concentration. (c) The overall change in "sensitivity" ($\Delta A_{523\,nm}/[H_2O_2]$) as a function of [BSA] added.

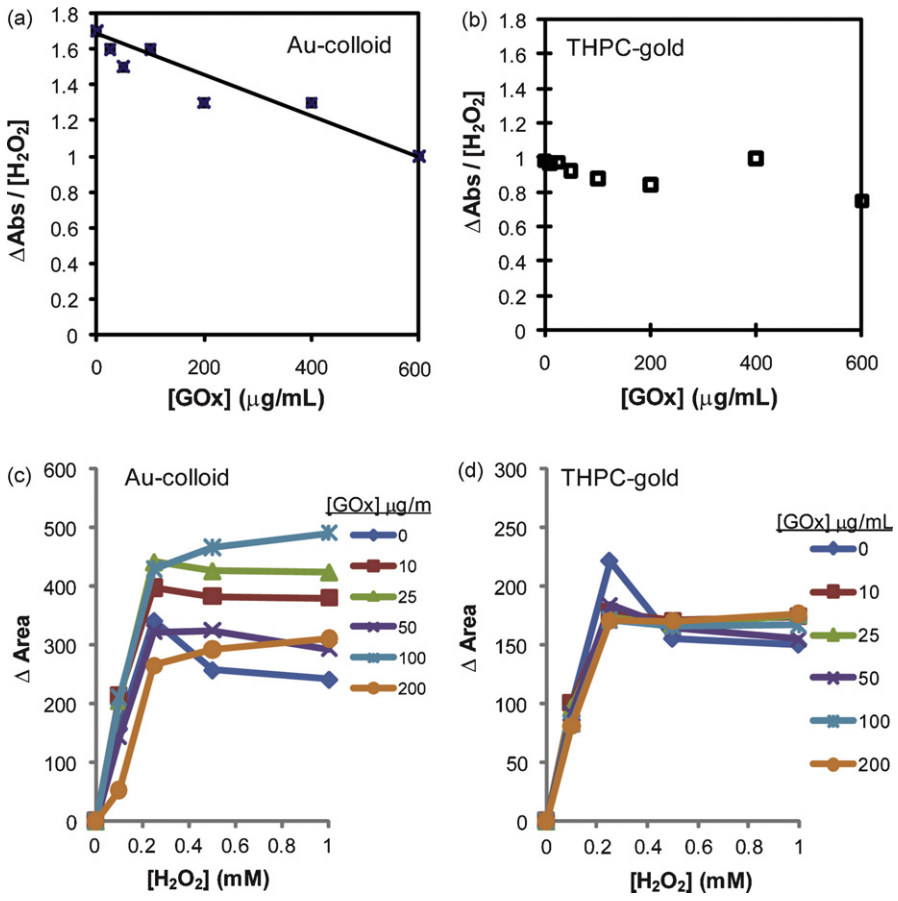

Fig. 5. Plots of the change in Abs at 523 nm versus $[H_2O_2]$ as a function of glucose oxidase addition for (a) Au-colloid and (b) THPC–gold. Plots of the change in area under the curve versus $[H_2O_2]$ for various concentrations of glucose oxidase added.

used in the detection of glucose (Fig. 5) in an analogous fashion to BSA. We find only limited reduction in the sensitivity of our model enzymatic sensor as a function of peroxidase concentration, even up to concentration levels of 600 μg/mL (Fig. 5a and b). However, it was clear from measuring the change in area under the curve as a function of GOx that the citrate-stabilized Au-colloid do have some change in response with the addition of GOx (Fig. 5c), though it was not as large as that seen with BSA. There is almost no difference seen for the THPC–gold particles using either change in absorbance at a single wavelength or overall area under the curve (Fig. 5b and d) as a measure of response. Our hypothesis is that glucose oxidase has a significantly lower affinity for the gold NPs than the serum albumin proteins.

4. Conclusions

In conclusion, the present study has demonstrated by employing UV–vis spectroscopy that the biocatalytic growth of Au-NPs is hindered due to the interaction between BSA and gold NPs. Electron microscopy and light scattering studies are consistent with the spectral data and suggest that BSA plays two roles in the seed mediated growth process. We propose a model in which protein attachment to the gold seed first prevents the detachment of nanoclusters from the seed particle surface and second leads to inhibition of surface catalytic sites. We are the first group to demonstrate that with the addition of a strongly bound protein with a high affinity to gold that this detachment can be prevented and change the overall morphology of the particles. Since numerous kinds of oxidases generate H_2O_2, this work reveals that biosensors based upon seed mediated catalysis will lose sensitivity in the presence of high concentrations of proteins with high affinity for the gold surface, such as BSA. However, large quantities of low affinity binding proteins, such as the enzyme itself, do not have a significant impact upon the catalytic ability of the nanoparticle surface even at significantly higher concentrations. This study provides insight into the design of biosensors based on seed mediated biocatalysis and the role that protein attachment can play in these studies.

Supplementary material

Detailed tables listing the TEM and DLS results are presented along with estimations of the packing density of BSA on the surface of the nanoparticles based on surface area and BSA put into the nanoparticle solutions. In addition, the changes in the area under the curve as a function of hydrogen peroxide and BSA and the slope of the change in peak area versus $[H_2O_2]$ is given. The change in slope for peak area versus hydrogen peroxide for both Au-colloid and THPC–gold is shown as a function of the number of BSA molecules per particle.

Acknowledgements

This work was supported through start-up funds provided to S.W.B by the College of Science and Letters at the Illinois Institute of Technology. Y.C. was supported through a scholarship provided by the China Scholarship Council. M.C. was supported through a fellowship provided by the Office of Undergraduate Research at IIT. K.F. was supported by NSF Illinois LSAMP Program—HRD 0413000. Transmission electron microscopy data was collected by Dr. Alan W. Nicholls at the Research Resource Center at the University of

Illinois at Chicago. Finally we thank our reviewers for very careful reading of the text and helpful suggestions in data analysis.

Appendix A. Supplementary data

Supplementary data associated with this article can be found, in the online version, at doi:10.1016/j.colsurfb.2009.10.043.

References

[1] J. Njagi, J. Warner, S. Andreescu, J. Chem. Educ. 84 (2007) 1180.
[2] W. Zhao, J.J. Xu, H.Y. Chen, Front. Biosci. 10 (2005) 1060–1069.
[3] A. Curulli, F. Valentini, G. Padeletti, A. Cusma, G.M. Ingo, S. Kaciulis, D. Caschera, G. Palleschi, Sens. Actuators B: Chem. 111 (2005) 526–531.
[4] L.R. Hirsch, J.B. Jackson, A. Lee, N.J. Halas, J. West, Anal. Chem. 75 (2003) 2377–2381.
[5] S. Lee, V.H. Perez-Luna, Langmuir 23 (2007) 5097–5099.
[6] K. Aslan, J.R. Lakowicz, C.D. Geddes, Anal. Chim. Acta 517 (2004) 139–144.
[7] L. Shang, H. Chen, L. Deng, S. Dong, Biosens. Bioelectron. 23 (2008) 1180–1184.
[8] M. Zayats, R. Baron, I. Popov, I. Willner, Nano Lett. 5 (2005) 21–25.
[9] I. Willner, R. Baron, B. Willner, Adv. Mater. 18 (2006) 1109–1120.
[10] J. Bai, K. Flowers, S. Benegal, M. Calizo, V. Patel, S.W. Bishnoi, J. Chem. Ed. 86 (2009) 712–714.
[11] N. Zhou, J. Wang, T. Chen, Z.G. Yu, G.X. Li, Anal. Chem. 78 (2006) 5227–5230.
[12] S.A. Kumar, M.K. Abyaneh, S.W. Gosavi, S.K. Kulkarni, R. Pasricha, A. Ahmad, M.I. Khan, Biotechnol. Lett. 29 (2007) 439–445.
[13] T.A. Taton, C.A. Mirkin, R.L. Letsinger, Science 289 (2000) 1757–1760.
[14] B. Abecassis, F. Testard, O. Spalla, P. Barboux, Nano Lett. 7 (2007) 1723–1727.
[15] J.H. Adair, E. Suvaci, Curr. Opin. Colloid Interface Sci. 5 (2000) 160–167.
[16] S.K. Bhargava, J.M. Booth, S. Agrawal, P. Coloe, G. Kar, Langmuir 21 (2005) 5949–5956.
[17] L.Y. Cao, T. Zhu, Z.F. Liu, J. Colloid Interface Sci. 293 (2006) 69–76.
[18] L. D'Souza, A. Suchopar, R.M. Richards, J. Colloid Interface Sci. 279 (2004) 458–463.
[19] N.R. Jana, L. Gearheart, C.J. Murphy, Chem. Mater. 13 (2001) 2313–2322.
[20] X.H. Ji, X.N. Song, J. Li, Y.B. Bai, W.S. Yang, X.G. Peng, J. Am. Chem. Soc. 129 (2007) 13939–13948.
[21] C.H. Kuo, T.F. Chiang, L.J. Chen, M.H. Huang, Langmuir 20 (2004) 7820–7824.
[22] Q. Liu, H. Liu, Q. Zhou, Y. Liang, G. Yin, Z. Xu, J. Mater. Sci. 41 (2006) 3657–3662.
[23] C. Note, S. Kosmella, J. Koetz, Colloids, Surf. A: Physicochem. Eng. Aspects 290 (2006) 150–156.
[24] R.G. Shimmin, A.B. Schoch, P.V. Braun, Langmuir 20 (2004) 5613–5620.
[25] R.R. Bhattacharjee, A.K. Das, D. Haldar, S. Si, A. Banerjee, T.K. Mandal, J. Nanosci. Nanotechnol. 5 (2005) 1141–1147.
[26] R. Levy, N.T.K. Thanh, R.C. Doty, I. Hussain, R.J. Nichols, D.J. Schiffrin, M. Brust, D.G. Fernig, J. Am. Chem. Soc. 126 (2004) 10076–10084.
[27] R.R. Naik, S.E. Jones, C.J. Murray, J.C. McAuliffe, R.A. Vaia, M.O. Stone, Adv. Funct. Mater. 14 (2004) 25–30.
[28] M. Sarikaya, C. Tamerler, D.T. Schwartz, F. Baneyx, Ann. Rev. Mater. Res. 34 (2004) 373–408.
[29] J.M. Slocik, M.O. Stone, R.R. Naik, Small 1 (2005) 1048–1052.
[30] Z. Wang, J.C. Chen, P. Yang, W.T. Yang, Appl. Organomet. Chem. 21 (2007) 645–651.
[31] A.C. Templeton, S.W. Chen, S.M. Gross, R.W. Murray, Langmuir 15 (1999) 66–76.
[32] J.L. Burt, C. Gutierrez-Wing, M. Miki-Yoshida, M. Jose-Yacaman, Langmuir 20 (2004) 11778–11783.
[33] M.P. Margarson, N.C. Soni, Br. J. Anaesth. 92 (2004) 821–826.
[34] S.H. Brewer, W.R. Glomm, M.C. Johnson, M.K. Knag, S. Franzen, Langmuir 21 (2005) 9303–9307.
[35] W.R. Glomm, O. Halskau, A.M.D. Hanneseth, S. Volden, J. Phys. Chem. B 111 (2007) 14329–14345.
[36] L. Shang, Y. Wang, J. Jiang, S. Dong, Langmuir (2007).
[37] N. Wangoo, C.R. Suri, G. Shekhawat, Appl. Phys. Lett. 92 (2008) 133103–133104.
[38] Zetasizer Nano Series User Manual, Malvern Instruments Ltd., Worcestershire, UK, 2005.
[39] P.C. Hiemenz, R. Rajagopalan, Principles of Colloid and Surface Chemistry, 3rd ed., Marcel Dekker, New York, 1997.
[40] X. Liu, M. Atwater, J. Wang, Q. Huo, Colloids Surf. B: Biointerfaces 58 (2007) 3–7.
[41] D.G. Duff, P.P. Edwards, A. Baiker, Langmuir 9 (1993) 2301–2309.
[42] K. Wang, J.J. Xu, H.Y. Chen, Biosens. Bioelectron. 20 (2005) 1388–1396.
[43] T. Sen, K.K. Haldar, A. Patra, J. Phys. Chem. C 112 (2008) 17945–17951.
[44] I. Willner, R. Baron, B. Willner, Biosens. Bioelectron. 22 (2007) 1841–1852.
[45] B. Lim, M. Jiang, P.H.C. Camargo, E.C. Cho, J. Tao, X. Lu, Y. Zhu, Y. Xia, Science (2009) 1170377.